J|A|C|S
COMMUNICATIONS

Published on Web 10/06/2007

Role of Electrostatic Interactions in Transient Encounter Complexes in Protein−Protein Association Investigated by Paramagnetic Relaxation Enhancement

Jeong-Yong Suh, Chun Tang, and G. Marius Clore*

Laboratory of Chemical Physics, National Institute of Diabetes and Digestive and Kidney Disease, National Institutes of Health, Bethesda, Maryland 20892-0520

Received August 13, 2007; E-mail: mariusc@mail.nih.gov

Protein−protein association can be viewed as a two-step process comprising the initial formation of an encounter complex ensemble followed by rearrangement, along a two-dimensional energy landscape, to form the final well-defined stereospecific complex (Figure 1).[1−5] Theoretical work suggests that electrostatic interactions play an important role in encounter complex formation, thereby enhancing molecular association by permitting a reduced dimensionality search until the stringent orientational requirements for specific association are met.[6] Recently, intermolecular paramagnetic relaxation enhancement (PRE) has been used to directly visualize an ensemble of lowly populated, highly transient encounter complexes in rapid exchange with the stereospecific complex.[3−5] In this exchange regime, the observed intermolecular PREs are weighted population averages of the PREs of the species present, and depending on paramagnetic center-proton distances, species with an occupancy as low as 1% can be detected.[3,4] For three relatively weak complexes ($K_D \sim 1-20\ \mu M$) from the bacterial phosphotransferase system, the distribution of nonspecific encounter complexes appeared to be qualitatively correlated to the electrostatic surface potentials of the interacting proteins.[4] In this paper, we extend our previous work on the complex of the N-terminal domain of enzyme I (EIN) and HPr[4,7] to examine the ionic strength dependence of intermolecular PREs and provide direct experimental evidence that the interactions involved in the formation of short-lived encounter complexes are predominantly electrostatic in nature.

NMR samples[4] comprised 0.3 mM U-[^{2}H/^{15}N]-EIN and 0.5 mM HPr in 20 mM Tris-HCl buffer, pH 7.4, with the concentration of NaCl ranging from 0 to 0.5 M. HPr was paramagnetically labeled with EDTA−Mn^{2+} conjugated via a disulfide linkage to surface-engineered cysteine residues at either position 5 (E5C) or 25 (E25C).[4] Intermolecular backbone ^1H_N PRE rates, Γ_2, for EIN were obtained by taking the difference in R_2 relaxation rates of paramagnetic and diamagnetic samples, measured at 40 °C using a TROSY-based pulse scheme[8] at a ^{1}H frequency of 600 MHz. The paramagnetic label at E25C of HPr is located relatively close to the binding interface of the stereospecific EIN/HPr complex (Figure 2C), while the label at E5C is located on the opposite surface of HPr (Figure 2A). The observed Γ_2 rates are weighted averages of the Γ_2 rates for the stereospecific complex and the ensemble of nonspecific encounter complexes.[4] The former is populated at ≥90%.[4] To a good approximation, the PREs can be readily partitioned into those arising from the stereospecific complex and those from the ensemble of nonspecific encounter complexes using the following criteria: (1) residues with $\Gamma_2 > 5\ s^{-1}$ for which there was no significant measurement error due to spectral overlap or line-broadening were selected for analysis; (2) observed Γ_2 rates in agreement with those back-calculated on the basis of the stereospecific complex[4] were attributed to the stereospecific complex (residues 115−125 for the EIN/E5C−HPr complex and residues 40−80 and 127−135 for the EIN/E25C−HPr complex), while the remainder were considered to originate primarily from the ensemble of nonspecific encounter complexes (residues 58−91 for the EIN/HPr−E5C complex, and residues 89−92 and 107−123 for the EIN/E25C−HPr complex) (Figure 2A,C).

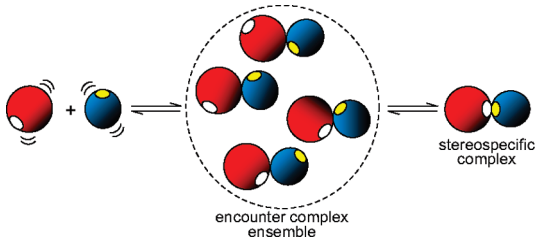

Figure 1. Protein−protein complex formation. The interaction surfaces involved in the stereospecific complex are shown in white and yellow.

The effect of salt on the magnitude of the PREs is displayed in Figure 2B (EIN/E5C−HPr) and 2D (EIN/E25C−HPr) as correlation plots of the Γ_2 rates at various salt concentrations versus the corresponding Γ_2 rates at 0 M NaCl. For the PREs attributed to the stereospecific complex, only a weak salt dependence is observed (top panels): the data at 0.15, 0.3, and 0.5 M NaCl versus 0 M NaCl exhibit slopes of 0.93 ± 0.01, 0.89 ± 0.03, and 0.86 ± 0.03 for the EIN/E5C−HPr complex, and 0.92 ± 0.02, 0.91 ± 0.02, and 0.85 ± 0.03 for the EIN/E25C−HPr complex, respectively. (The corresponding correlation coefficients are 0.99, 0.92, 0.94, 0.97, 0.98, and 0.96.) For the PREs attributed to the ensemble of nonspecific encounter complexes, however, a much larger salt dependence is observed with values of the slopes for the 0.15, 0.3, and 0.5 M NaCl data versus 0 M NaCl data of 0.90 ± 0.03, 0.71 ± 0.02, and 0.63 ± 0.03, respectively, for the EIN/E5C−HPr complex, and 0.84 ± 0.05, 0.69 ± 0.04, and 0.60 ± 0.05, respectively, for the EIN/E25C−HPr complex. (The corresponding correlation coefficients are 0.98, 0.98, 0.96, 0.88, 0.86, and 0.79, respectively.) Importantly, the observed salt dependencies are the same within experimental error for the data obtained on both the EIN/E5C−HPr and EIN/E25C−HPr complexes, indicating that the data from the two samples are reporting on the same overall interactions.

The decrease in magnitude of the PREs arising from the stereospecific complex as a function of salt is attributable to an increase in equilibrium dissociation constant, K_D (largely due to a decrease in the association rate constant[6d]), and hence decrease in the population of stereospecific complex as the salt concentration increases, as confirmed by isothermal titration calorimetry (ITC) experiments (see Supporting Information for details). As is evident from Figure 3A, the log−log plot of K_D versus NaCl concentration shows the expected linear dependence over the 0.15−2 M NaCl range.[9] Under the conditions of the NMR experiments, this translates

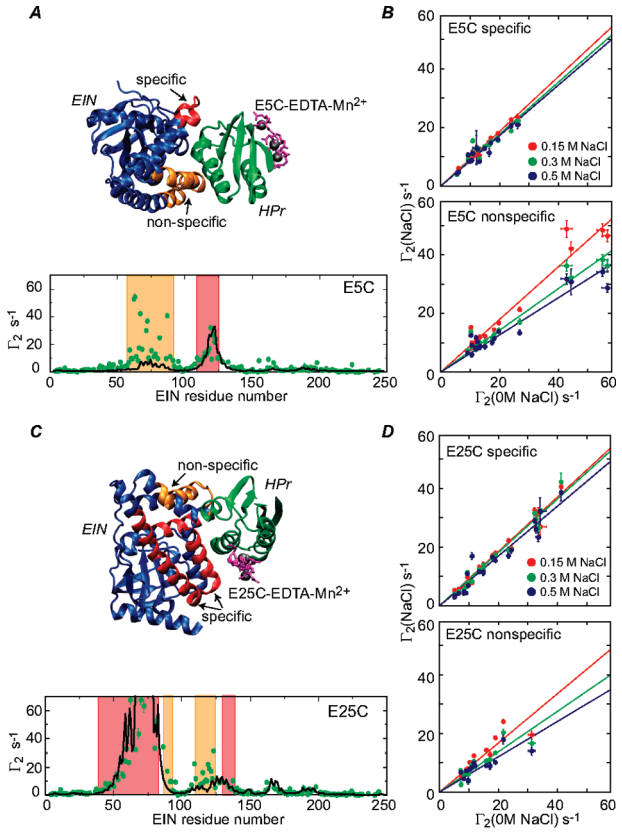

Figure 2. Ionic strength dependence of intermolecular PREs for the EIN/HPr complex. (A and C) Structure of the EIN(blue)/HPr(green) stereospecific complex[7c] (top panels) with EDTA−Mn^{2+} conjugated to E5C and E25C, respectively, displayed as a three-conformer ensemble. Intermolecular PREs attributable to interactions involving the stereospecific complex (red) and the ensemble of nonspecific encounter complexes (orange) are displayed on the structure (top panels) and highlighted on the PRE profiles (bottom panels). The experimental Γ_2 rates (at 0 M NaCl) are shown as green circles, and the Γ_2 rate profiles back-calculated from the structure of the stereospecific complex[4] are shown as continuous black lines. (B and D) Correlation of Γ_2 rates arising from the stereospecific complex (top panels) and the ensemble of nonspecific encounter complexes (bottom panels) at 0.15 (red), 0.3 (green), and 0.5 (blue) M NaCl versus the corresponding Γ_2 rates at 0 M NaCl for (B) EIN/HPr−E5C and (D) EIN/HPr−E25C.

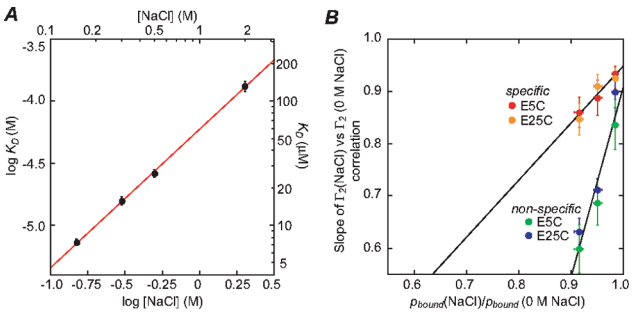

Figure 3. (A) Ionic strength dependence of the K_D for the EIN/HPr complex determined by ITC. (B) Dependence of the slopes of the Γ_2(NaCl) versus Γ_2(0 M NaCl) correlations (from Figure 2) versus the normalized bound population, p_{bound}(NaCl)/p_{bound}(0 M NaCl), of stereospecific complex, derived from the K_D values determined by ITC.

to a bound population, p_{bound}, expressed as a percentage of total EIN concentration, of 98.2, 96.6, 93.3, and 89.8% at 0, 0.15, 0.3, and 0.5 M NaCl, respectively. Plots of the slope of the linear regression line for the Γ_2(NaCl) versus Γ_2(0 M NaCl) correlations against the bound population normalized to that at 0 M NaCl, p_{bound}(NaCl)/p_{bound}(0 M NaCl), reveal two distinct correlations, one for the PRE data arising from the stereospecific complex and the other for the ensemble of nonspecific encounter complexes. For the former, the slope is very close to unity (1.1 ± 0.15, with a correlation coefficient of 0.96), confirming that the decrease in PRE magnitude for the stereospecific complex is directly related to the population of the stereospecific complex derived from the ITC data; for the latter, however, the slope is a factor of 3.3-fold higher (slope = 3.6 ± 0.5, correlation coefficient = 0.96), indicating that the nonspecific encounter complexes are significantly more sensitive to ionic strength than the stereospecific complex.

The data presented in this paper clearly demonstrate that the population of nonspecific encounter complexes is modulated by ionic strength to a larger degree than the stereospecific complex, highlighting the importance of electrostatic interactions in the formation of the nonspecific encounter complex ensemble. These results are consistent with Debye−Hückel theory[10] since the average intermolecular distance between oppositely charged residues is expected to be significantly longer in the nonspecific encounter complex ensemble than in the stereospecific one. In particular, the nonspecific interfaces are much less compact than the stereospecific one, as measured by the gap index (ratio of buried accessible surface area to gap volume) which ranges from 5 to 50 times larger for the nonspecific encounter complexes than the stereospecific complex.[4] Thus, ions in solution can more effectively screen intermolecular electrostatic interactions in the loosely packed nonspecific encounter complexes than in the tightly bound stereospecific complex because the former are more accessible to ions than the latter.

Acknowledgment. This work was supported by the Intramural Program of NIDDK, NIH, and the AIDS Targeted Antiviral program of the Office of the Director of the NIH (to G.M.C.). We thank A. Szabo for useful discussions.

Supporting Information Available: ITC data for the binding of HPr to EIN at various salt concentrations. This material is available free of charge via the Internet at http://pubs.acs.org.

References

(1) (a) Berg, O. G.; von Hippel, P. H. *Annu. Rev. Biophys. Biophys. Chem.* **1985**, *14*, 131−160. (b) Schrieber, G.; Fersht, A. R. *Nat. Struct. Biol.* **1996**, *3*, 427−431. (c) Vijayakumar, M.; Wong, K.-Y.; Schreiber, G.; Fersht, A. R.; Szabo, A.; Zhou, H.-X. *J. Mol. Biol.* **1998**, *278*, 1015−1024. (d) Selzer, T.; Albeck, S.; Schreiber, G. *Nat. Struct. Biol.* **2000**, *7*, 537−541.
(2) Blundell, T. L.; Recio-Fernandez, J. *Nature* **2006**, *444*, 279−280.
(3) Iwahara, J.; Clore, G. M. *Nature* **2006**, *440*, 1227−1230.
(4) Tang, C.; Iwahara, J.; Clore, G. M. *Nature* **2006**, *444*, 383−386.
(5) Volkov, A. N.; Worall, J. A. R.; Holtzmann, E.; Ubbink, M. *Proc. Natl. Acad. Sci. U.S.A.* **2006**, *103*, 18945−18950.
(6) (a) Northrup, S. H.; Boles, J. O.; Reynolds, J. C. L. *Science* **1988**, *241*, 67−70. (b) Spaar, A.; Dammer, C.; Gabdouille, R. R.; Wade, R. C.; Helms, V. *Biophys. J.* **2006**, *90*, 1913−1924. (c) Zhou, H.-X.; Szabo, A. *Phys Rev. Lett.* **2004**, *93*, 178101. (d) Zhou, H.-X. *Biopolymers* **2001**, *59*, 427−433.
(7) (a) Garrett, D. S.; Seok, Y. J.; Liao, D. I.; Peterkofsky, A.; Gronenborn, A. M.; Clore, G. M. *Biochemistry* **1997**, *36*, 2517−2530. (b) Garrett, D. S.; Seok, Y.-J.; Peterkofsky, A.; Clore, G. M.; Gronenborn, A. M. *Biochemistry* **1997**, *36*, 4393−4398. (c) Garrett, D. S.; Seok, Y.-J.; Peterkofsky, A.; Gronenborn, A. M.; Clore, G. M. *Nat. Struct. Biol.* **1999**, *6*, 166−173.
(8) (a) Iwahara, J.; Schwieters, C. D.; Clore, G. M. *J. Am. Chem. Soc.* **2004**, *126*, 5879−5896. (b) Iwahara, J.; Tang, C.; Clore, G. M. *J. Magn. Reson.* **2007**, *184*, 185−195.
(9) Record, M. T., Jr.; Lohman, T. M.; de Haseth, P. *J. Mol. Biol.* **1976**, *107*, 145−158.
(10) McQuarrie, D. A. *Statistical Mechanics*; University Science Books: Mill Valley, CA, 2000; Chapter 15, pp 326−351.

JA0760978